

Learning Sequential Contexts using Transformer for 3D Hand Pose Estimation

Leyla Khaleghi, Joshua Marshall, Ali Etemad

Dept. ECE and Ingenuity Labs Research Institute

Queen’s University

Kingston, ON, Canada

{leyla.khaleghi, joshua.marshall, ali.etemad}@queensu.ca

Abstract—3D hand pose estimation (HPE) is the process of locating the joints of the hand in 3D from any visual input. HPE has recently received an increased amount of attention due to its key role in a variety of human-computer interaction applications. Recent HPE methods have demonstrated the advantages of employing videos or multi-view images, allowing for more robust HPE systems. Accordingly, in this study, we propose a new method to perform Sequential learning with Transformer for Hand Pose (SeTHPose) estimation. Our SeTHPose pipeline begins by extracting visual embeddings from individual hand images. We then use a transformer encoder to learn the sequential context along time or viewing angles and generate accurate 2D hand joint locations. Then, a graph convolutional neural network with a U-Net configuration is used to convert the 2D hand joint locations to 3D poses. Our experiments show that SeTHPose performs well on both hand sequence varieties, temporal and angular. Also, SeTHPose outperforms other methods in the field to achieve new state-of-the-art results on two public available sequential datasets, STB and MuViHand.

I. INTRODUCTION

Various human-computer interaction applications including gaming, autonomous driving, automatic sign-language recognition, and others, rely upon the estimation of hand joint locations—i.e., hand pose estimation (HPE)—from input visual data [1], [2], [3]. Despite the considerable improvements in HPE methods with the help of deep learning [4], [5], many methods still struggle to deal with challenges such as occlusions (which could happen by a body part or by a part of the hand itself, called self-occlusion), large number of possible hand poses (large pose space), large number of hand shapes, various skin colors, and sharp camera viewpoints.

So far, the majority of HPE solutions focus on using single RGB images as inputs [6], [7], [8], [9], [10], [11], [12], [13], [14], [15], [16], [17], [18], [19], [20], [21], [22], overlooking the information in the sequential structure of the hand in time and/or across different views. Thus far, only a few studies [23], [24], [25] have considered the temporal relations of hand frames in videos to improve the performance of HPE. Similarly, only a few methods [25], [26] have fused multi-view hand images to capture the geometric relations among different viewpoints and improve HPE performance.

Despite sequential information (time/view) often being ignored for HPE, we believe their effective learning and aggregation could lead to more robust contextualized representations and ultimately more accurate HPE. While recurrent neural

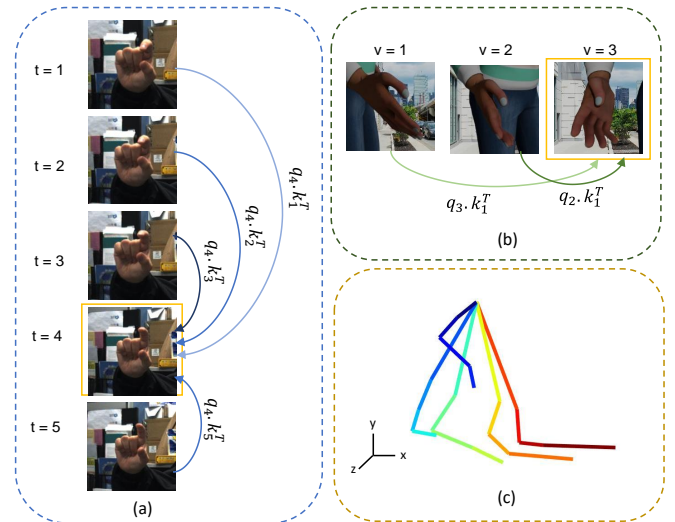


Fig. 1. SeTHPose scores the relevancy of each pair of hand images in a sequence (time/view) according to its surrounding context with a self-attention mechanism to estimate the corresponding 3D hand pose.

networks have been used in the past for learning such time/view contextual information [25], [23], the Transformer self-attention [27], which has recently shown remarkable results in various computer vision tasks [28], [29], [30], appears to be a strong candidate for learning sequential information across time or views for enhancing 3D HPE. As a result, we propose a new HPE method called Sequential learning with Transformer for Hand Pose (SeTHPose) estimation. Our model first uses a CNN encoder to generate the spatial embeddings for each hand frame, followed by a transformer encoder to learn the contextual relations of the hand embeddings across time or views (Figures 1(a) and (b) demonstrate the different contextual data types, while (c) demonstrates a sample 3D pose output). Next, an MLP is used for estimating the 2D hand joint locations. This is followed by a graph convolutional U-network to convert the learned 2D structures to 3D hand joint locations. We validate our model on two publicly available *sequential* datasets, STB [31] and MuViHand [25], and achieve state-of-the-art results by outperforming previous works in the area. Moreover, we perform additional experiments, such as ablation studies, to

evaluate the impact of contextual learning within our model. While a few new techniques have been recently proposed to use transformers for HPE [12], [13], [14], their use has been solely limited for obtaining better single-image embeddings or joint locations, while our method uses the transformer component to learn the contextual information across time or view sequences. To the best of our knowledge, SeTHPose is the first method that learns *sequential contextual information* with transformer for 3D HPE.

Our contributions in this paper are summarized as follows:

- We propose SeTHPose, a method for strong 3D hand pose estimation. Our method relies on a transformer to learn contextual sequential information and produce better 2D joint locations, which are then converted to 3D using a graph convolutional U-Net.
- Our experiments show that SeTHPose works for two different types of sequential information, namely time and camera angles.
- SeTHPose outperforms existing techniques in the area to achieve state-of-the-art results on two public datasets, STB and MuViHand.

We have organized the remainder of this paper as follows. A literature review on recent HPE methods is explained in Section 2. We introduce our proposed method in Section 3 in detail. Our experiments and results on SeTHPose are presented in Section 4. Finally, Section 5 provides the concluding remarks.

II. RELATED WORK

In this study, we focus primarily on 3D HPE by exploiting sequential contexts; i.e., both temporal and angular. Accordingly in this section we review typical HPE techniques that rely on single images (non-sequential), as well as approaches that exploit either temporal and/or angular contexts (sequential).

A. Non-Sequential HPE

In some prior HPE literature, estimating 2D hand locations had been used as an intermediary step for estimating 3D poses from RGB images. In [6], a 2D heatmap was generated directly from an image embedding for each hand joint, and a normalized 3D hand coordinate was then calculated from the 2D heatmap. Similarly, in [7], the depth data was measured in addition to the initial 2D heatmaps, from which the 3D hand pose was calculated. In comparison to [6] and [7], [8] is a two-stage approach to 3D hand pose estimation. The 2D joint locations were estimated rather than the 2D heatmaps, and the 3D hand pose was determined from the joint locations via a graph-based network.

The MANO hand model [32] was employed in multiple HPE techniques for estimating hand poses. MANO maps two parameters, namely pose (joint angles) and shape (individual deformations of the hands), to a 3D hand mesh. In [9], MANO hand parameters were directly derived from the image embeddings obtained from a ResNet18. In [10], MANO parameters were estimated based on 2D heatmaps and using hand mask supervision, calculated through hand vertices. In [11], the MANO parameters were calculated by providing

an RGB image and its corresponding 2D hand joints to a ResNet50.

A few HPE pipelines have employed the self-attention transformer mechanism. In [12], image embeddings along with 2D hand keypoint heatmaps were fed to a transformer in order to calculate the 3D hand positions. In [13], hand images were fed to a ResNet encoder to generate hand joints in 2D, which were then passed through a transformer to estimate hand poses in 3D. In [14], encoded hand images were passed through a multilayer transformer in order to regress the 3D hand poses.

B. Sequential HPE

Exploiting sequential contextual information, either in the form of consecutive video frames or multi-view images, has rarely been studied in HPE literature. In [23], an LSTM layer followed image encoders to learn the temporal relationships between the consecutive hand images and generate the parameters for the MANO hand model for each frame. In [24] the temporal relationships between 2D hand joint locations were considered through GC layers with extra edges between the exact hand joints in the following frames, where state-of-the-art methods such as OpenPose [33] could be used to estimate the 2D hand joint locations. In [26], a single-view HPE generated 3D camera coordinates for different views using multiple hand images. A graph-based structure then calculated the world coordinate by concatenating the camera coordinates.

The only approach, in the literature that could learn both angular and temporal relationships for HPE is [25]. In this paper, the 2D locations of the hand joints were generated by two LSTM layers that jointly learned the relevance of hand videos captured from multiple perspectives. By using GC layers that allowed for learning of hand joints' relevancy, the 3D hand pose could be estimated from the 2D hand joint locations.

Despite the promising results obtained by transformers in other domains, there are currently no HPE approaches that examine the utility of transformer encoders for learning sequential contexts of hand data. This motivates our study where we present SeTHPose, the first sequential transformer-based 3D HPE method.

III. METHOD

A. Problem Setup and Solution Overview

Our work is based on the idea of considering the temporal or angular contextual information in hand sequences as a practical solution for improving the performance of HPE [23], [24], [25], [26]. Accordingly, we can denote our proposed method SeTHPose using ζ , which can predict 3D hand poses from the corresponding hand sequence φ , such that

$$P = \zeta[\varphi], \quad (1)$$

where φ is a sequence of RGB hand frames $\in \mathbb{R}^{N \times 3 \times H \times W}$, N is the sequence length, H is the image height, and W is the image width. Moreover, $P \in \mathbb{R}^{N \times j \times 3}$ is the sequence of corresponding 3D hand poses that could describe N hand skeletons, each consisting of j joints. A sample output 3D hand pose can be seen in Figure 1(c).

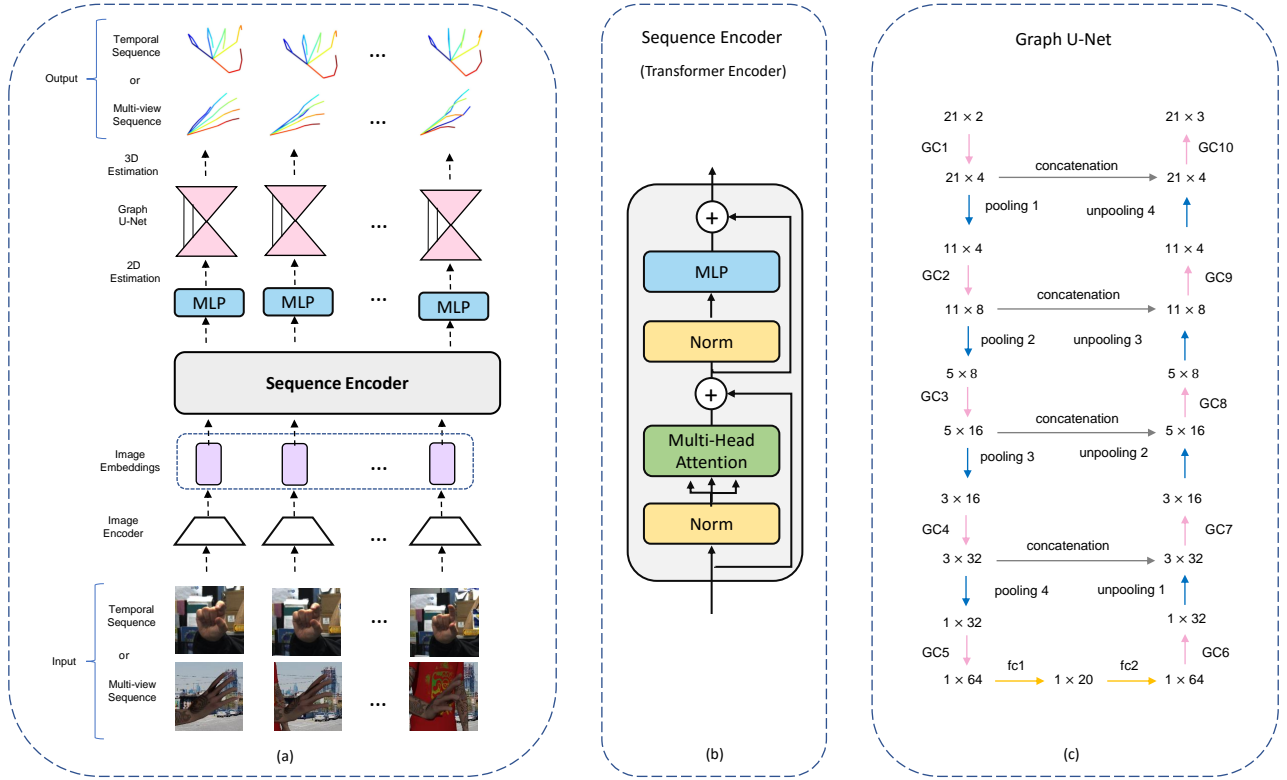


Fig. 2. This diagram illustrates the pipeline for SeTHPose. An image encoder, a sequence encoder, and Graph U-Nets constitute the model. Transformer encoders take N image embeddings in time or view from ResNet10. Afterward, an MLP that estimates 2D coordinates is applied to each encoder’s output. In the next step, a Graph U-Net calculates the 3D hand pose from the corresponding 2D joint locations for each frame.

Figure 2(a) provides an overview of the proposed network. In our model, a ResNet is first used to encode the input images and produce individual hand frame embeddings. Then, inspired by recent works in other fields of computer vision that have used transformers to learn sequential information across time [34], [35] or space [36], [37], we use a transformer encoder to learn the contextual sequential (temporal or angular) information. The output of the transformer is then used to produce 2D hand joint locations. SeTHPose then passes the estimated 2D joints to a Graph U-Net to estimate the 3D hand poses. In the following sub-sections we discuss each of the main components of SeTHPose in detail.

B. Image Encoding

In this research, we use a ResNet10 [38] pre-trained on ImageNet [39] to generate the image embeddings for each hand frame. Our encoder takes each hand frame ϕ_i and generates an image embedding $x_i \in \mathbb{R}^{1 \times f}$, where $i = 1, 2, \dots, N$. By design, this encoder does not incorporate contextual sequential information because it only focuses on single frames. Thus, we need another component in our model to combine the individual embeddings in order to learn the surrounding context for each input frame. This leads to the use of a transformer encoder in SeTHPose, which we describe in the following sub-section.

C. Sequence Encoding

To exploit the sequence of embeddings obtained from individual frames and eventually generate contextually-informed poses, we use a transformer encoder. Given an input $X \in \mathbb{R}^{N \times f}$, for each image embedding $x_i \in \mathbb{R}^{1 \times f}$, linear transformations $w_q \in \mathbb{R}^{f \times d_q}$, $w_k \in \mathbb{R}^{f \times d_k}$, and $w_v \in \mathbb{R}^{f \times d_v}$ are calculated. These values will map x to queries $q = xw_q$, keys $k = xw_k$, and values $v = xw_v$. Here, d_q , d_k , and d_v , are the embedding dimensions.

To provide the relevancy of each image embedding x_i based on other image embeddings available in the sequence x_j , $i, j = 1, 2, \dots, N$, we calculate relevancy score $s_{ij} = q_i k_j^T$. Next, by summing the multiplication of value vectors v_j with s_{ij} , and normalizing the output with a softmax function, the new feature embedding for each image is calculated. This objective is named Scaled Dot-Product Attention [27] which is formulated as

$$\text{Attention}(Q, K, V) = \text{softmax} \left(\frac{QK^T}{\sqrt{d_k}} \right) V, \quad (2)$$

where, d_k acts as a scaling factor to improve gradient stability during training.

The use of multi-headed attention is a common strategy to improve the performance of the transformer where the attention mechanism is applied H times with distinct learnable

parameters according to

$$\text{head}_h = \text{Attention}(QW_h^Q, KW_h^K, VW_h^V), \quad (3)$$

where $h = 1, 2, \dots, H$. The final result, MH , is calculated as

$$MH(Q, K, V) = \text{concat}(\text{head}_1, \dots, \text{head}_h)W_{out}. \quad (4)$$

We utilize a multi-head self-attention mechanism to generate new hand image embeddings based on the sequential context (time or view) between the hand frames (see Figures 1(a) and 1(b) for examples). Ultimately, N set of features $c_i \in \mathbb{R}^{1 \times L}$, where L is the transformer’s output feature size, is generated in this stage to be fed into an MLP to produce the corresponding 2D hand joint locations $z_i \in \mathbb{R}^{21 \times 2}$, for N hand frames.

D. 2D to 3D Pose Conversion

As a next step, we convert the set generated 2D hand poses to 3D poses using a Graph U-Net, which consists of Graph Convolutional (GC) layers, as shown in Figure 2(c). Since the hand skeleton consists of a graph structure, the GC layers have been found to perform well for HPE [8], [22], [24], [25], [26].

For each GC layer, a graph $G = (K, A)$, with K nodes and $A \in \mathbb{R}^{K \times K}$ as the adjacency matrix is defined. As per earlier research [8], [25], we select a learnable adjacency matrix that has shown to achieve more effective results than predefined adjacency matrices. By feeding an input $X \in \mathbb{R}^{K \times F}$ to each GC layer, an output vector $O \in \mathbb{R}^{K \times E}$ is generated

$$O = \sigma(\bar{A}XW), \quad (5)$$

where F and E are the input and output feature sizes respectively, and $W \in \mathbb{R}^{E \times L}$ is the trainable weight matrix. \bar{A} is the normalized adjacency matrix [40] of G , which is measured as

$$\bar{A} = D^{-\frac{1}{2}} \hat{A} D^{-\frac{1}{2}}, \quad (6)$$

where D is defined as the diagonal node degree matrix of G . Here \hat{A} is calculated according to

$$\hat{A} = A + I, \quad (7)$$

where I is the identity matrix.

The Graph U-Net module is formed by multiple GC layers situated in a U-net encoder-decoder architecture with several skip connections between the corresponding layers. Finally, the Graph U-net converts each set of 2D hand joint locations $z_i \in \mathbb{R}^{21 \times 2}$ to its corresponding 3D hand pose $p_i \in \mathbb{R}^{21 \times 3}$.

E. Training and Loss Function

We take two steps for training SeTHPose. First (Step 1), The pipeline is trained regardless of the sequence encoder. During this process, the transformer encoder is temporarily replaced by a fully connected layer. By doing so, we effectively implement HPE on every frame by optimizing the loss function

$$L = \alpha L_{2D} + L_{3D}, \quad (8)$$

where α is set to 0.1, and L_{2D} is defined as

$$L_{2D} = \|\hat{z} - z\|_2, \quad (9)$$

TABLE I
PERFORMANCE COMPARISON BETWEEN SeTHPOSE AND OTHER METHODS ON STB DATASET.

Method	Input Data	↓ Avg. EPE	↑AUC (20-50)
Zhang et al. [31] (PSO)	Image	-	0.709
Zhang et al. [31] (ICPPSO)	Image	-	0.748
Zhang et al. [31] (CHPR)	Image	-	0.839
Panteleris et al. [18]	Image	-	0.941
Zimmerman & Brox [6]	Image	-	0.948
Mueller et al. [17]	Video	-	0.965
Spurr et al. [16]	Image	8.56	0.983
Yang et al. [23]	Image	9.80	0.985
Chen et al. [19]	Image	9.11	0.990
Yang et al. [20]	Image	8.66	0.991
Li et al. [21]	Image	-	0.996
Iqbal et al. [7]	Image	-	0.994
SeTHPose (Ours)	Video	7.841	0.998

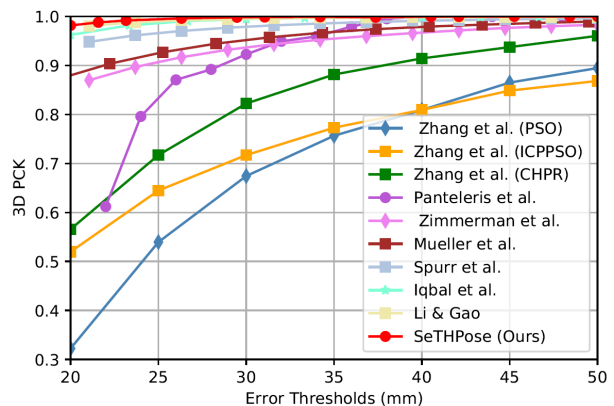


Fig. 3. The comparison of 3D PCK curve of our proposed method against other solutions [31], [18], [6], [17], [16], [7], [21] on STB dataset.

and \hat{z} and z are the predicted and ground truth 2D coordinates respectively. Similarly, the L_{3D} is calculated according to

$$L_{3D} = \|\hat{p} - p\|_2, \quad (10)$$

where \hat{p} and p are the predicted and ground truth 3D coordinates, respectively. Following this, in Step 2, we freeze the image encoder and train the complete SeTHPose pipeline, effectively re-training the Graph U-Net and MLP, and training the sequence encoder (transformer encoder). Here, we use the loss function

$$L = \frac{1}{N} \sum_N \|\hat{p}_i - p_i\|_2. \quad (11)$$

IV. EXPERIMENTS AND RESULTS

A. Datasets

We use two publicly available 3D HPE datasets, STB [31] and MuViHand [25]. We specifically select these datasets because they both contain hand poses in *video* or *multi-view* formats. Two other datasets, MVHM [26] and SeqHand [23], which also contain multi-view and video-based data, could also have been used for this study, but the respective datasets were not made public at the time that we carried out our work. Next we describe the two datasets used in this study.

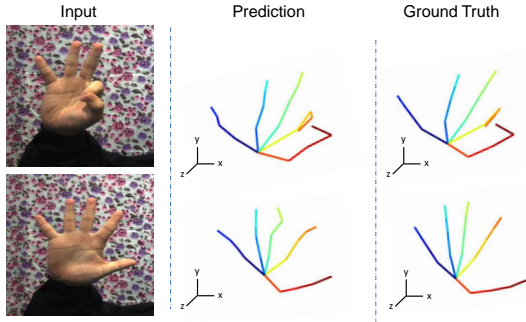


Fig. 4. Sample visualization using SeTHPose for the STB dataset.

TABLE II
PERFORMANCE COMPARISON BETWEEN SeTHPOSE AND OTHER METHODS ON MUVIHAND DATASET WITH TWO DIFFERENT TESTING PROTOCOLS.

Test	Method	Input Data	↓ Avg. EPE	↑AUC
cross-subject	Boukhayma et al. [11]	Image	48.840	0.280
	Hasson et al. [9]	Image	28.915	0.574
	Doosti et al. [8]	Image	18.895	0.634
	Khaleghi et al. [25]	Video	11.82	0.766
	Khaleghi et al. [25]	Multi-view Images	10.034	0.808
	Khaleghi et al. [25]	Multi-view Videos	8.881	0.831
	SeTHPose _t (Ours)	Video	7.697	0.846
	SeTHPose _v (Ours)	Multi-view Images	7.384	0.861
cross-activity	Boukhayma et al. [11]	Image	42.799	0.287
	Hasson et al. [9]	Image	66.851	0.152
	Doosti et al. [8]	Image	46.745	0.217
	Khaleghi et al. [25]	Video	23.631	0.557
	Khaleghi et al. [25]	Multi-view Images	21.463	0.592
	Khaleghi et al. [25]	Multi-view Videos	20.375	0.608
	SeTHPose _t (Ours)	Video	18.607	0.638
	SeTHPose _v (Ours)	Multi-view Images	17.616	0.657

Stereo Hand Pose Tracking Benchmark (STB) [31] is a single-view real-world dataset that captures 12 hand *videos*. We use the same training/test splits as previous studies [11], [16], [19], [23], training the model on ten videos and testing it on the remaining videos.

Multi-view video based Hand (MuViHand) [25] is a synthetic dataset containing video footage of 10 subjects performing 17 activities from multiple perspectives. In this study, we use the same train/test protocol as in the original paper. Specifically, in the cross-subject protocol, we train on subjects 3, 4, ..., 9 and test on subjects 1, 2, 10, while in the cross-activity protocol, we train on activities 1, 2, ..., 7, 9, 10, ..., 18, and test on activities 8, 19.

B. Metrics

Following the standard protocols used for HPE[6], we calculate three metrics for evaluating our method. These metrics are (i) mean endpoint error (EPE), (ii) the proportion of correct keypoints whose Euclidean distance error is less than a threshold (3D PCK), and (iii) the area under the curve of the 3D PCK (AUC). It should be noted that the threshold for 3D PCK is selected similar to previous works in the area [6], [7], [16], [17], [18], [21], [31], [25].

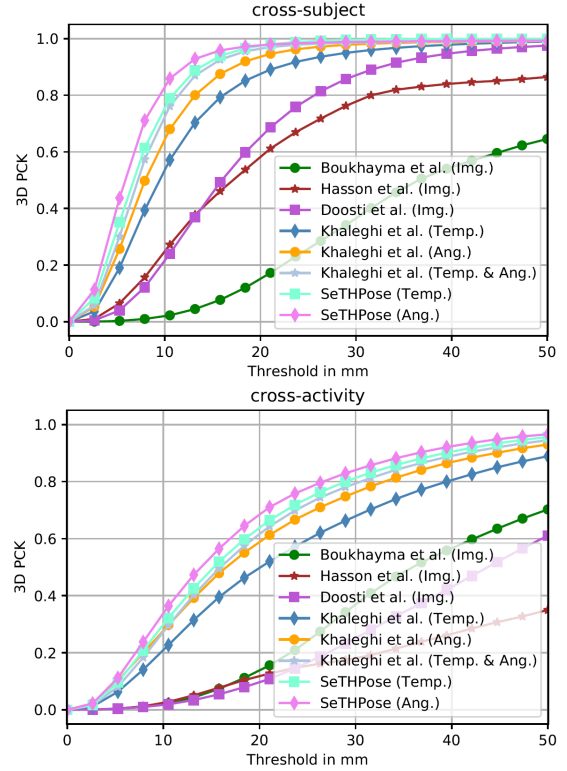


Fig. 5. The comparison of 3D PCK curve of our proposed method against other solutions [11], [9], [8], [25] on two testing protocols of MuViHand dataset; top: cross-subject and bottom: cross-activity.

C. Implementation Details

The two datasets used in this study contain different types of data. STB is a real dataset containing temporal sequences, while MuViHand is a synthetic dataset containing both temporal and angular sequences. Thus, the training parameters used for the two datasets are different to accommodate for the varying levels of difficulty and synthetic versus real nature of the data. We implement our model using PyTorch and perform the training on an Nvidia GeForce GTX 2070 Ti GPU.

For training with the STB dataset, in Step 1, we use an initial learning rate of 0.005, and decrease it by a factor of 0.09 every 50 epochs for 500 epochs. Following this, in Step 2, we train SeTHPose with $N = 5$ for 5000 iterations at an initial learning rate of 0.001, multiplied by 0.95 every 50 iterations.

Given that MuViHand dataset contains both temporal (video) data and multi-view images, we explore both temporal and angular relationships using our model. Accordingly we have SeTHPose_t and SeTHPose_v, which refers to two separate experiments, one for learning temporal relationships and the other for learning angular relationships. In Step 1 of training, we train both variations for 500 epochs at an initial learning rate of 0.001, multiplied by 0.1 after every 100 epochs. Afterwards, SeTHPose_t is trained with $N = 5$ while SeTHPose_v is trained with $N = 3$ with an initial learning rate of 0.001, is multiplied by 0.9 every 100 epochs for 350 epochs.

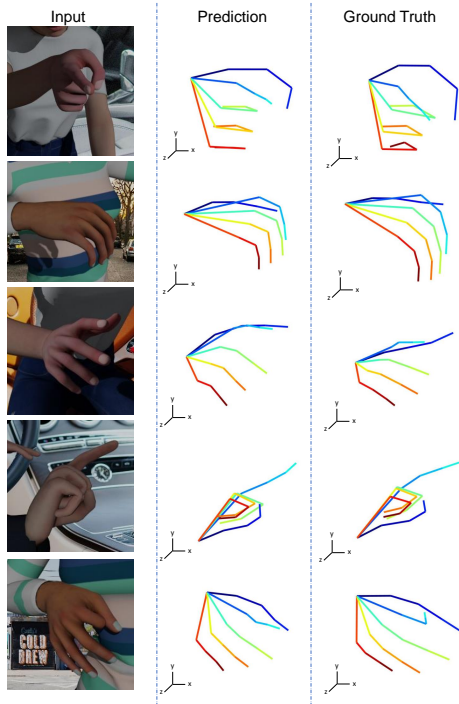


Fig. 6. Sample visualization using SeTHPose for the MuViHand dataset.

D. Performance and Discussion

We evaluate and compare the performance of SeTHPose on STB dataset against other state-of-the-art single-image HPE methods [6], [7], [16], [17], [18], [19], [20], [21], [31] and the only video-based method available in the literature on this particular dataset [23]. We present this comparison in Table I. The performance values have been obtained from the original papers (in some cases the EPE metric has not been reported). SeTHPose shows excellent performance on STB with no additional training data in contrast to [19], [20], [23], which rely on training on several datasets for better generalization. Furthermore, in Figure 3, we present the 3D PCK curves of our method in comparison to [6], [7], [16], [17], [18], [21], [31] for different thresholds (20-50). Also, in Figure 4, we illustrate several samples of input images and output poses estimated by SeTHPose.

We present the results of SeTHPose (both SeTHPose_t and SeTHPose_v) on MuViHand dataset and compare the performances against [8], [9], [11] as well as two additional variations of [25]. Interestingly, both variations of our method outperform all other existing methods on this dataset, including both multi-view and video-based methods. A graph showing the PCK curves for thresholds 0 to 50 for our method and other methods is presented in Figure 5 for both test protocols. Also, in Figure 6, we illustrate multiple examples of our network’s performance on the MuViHand dataset.

To evaluate the sensitivity of our method against the number of attention heads H , we repeat the experiments with different variations of the transformer-based sequence encoder by setting

TABLE III
IMPACT OF H WHICH IS USED IN THE TRANSFORMER ENCODER IN THE SETHPOSE ON THE EPE.

Dataset	Method	H					
		1	2	4	8	16	
STB	SeTHPose	10.034	9.406	9.069	7.841	8.787	
MuVi.	sub.	SeTHPose _t	8.878	8.328	8.159	7.697	7.825
		SeTHPose _v	8.504	7.842	7.264	7.384	7.805
	act.	SeTHPose _t	19.384	18.648	19.424	18.607	19.171
		SeTHPose _v	20.043	17.287	17.837	17.616	16.708

TABLE IV
ABLATION RESULTS ON SETHPOSE.

Dataset	Method	Temporal	Angular	↓ Avg. EPE	↑ AUC	
STB	Ablation	✗	✗	32.450	0.600	
	SeTHPose	✓	✗	7.841	0.998	
MuViHand	cr.-sub.	Ablation	✗	✗	14.529	0.723
		SeTHPose _t	✓	✗	7.697	0.846
	SeTHPose _v	✗	✓	7.384	0.861	
	cr.-act.	Ablation	✗	✗	44.021	0.246
SeTHPose _t		✓	✗	18.607	0.638	
SeTHPose _v	✗	✓	16.708	0.657		

H to 1, 2, 4, 8, and 16. We present the results in TableIII, where we observe that 4, 8, and 16 attention heads achieve relatively close results. Yet, $H = 8$ provides slightly better overall performance, which was selected for our model.

E. Ablation Study

To explore the impact of the transformer encoders on learning the sequential contexts in our method, we perform ablation studies on SeTHPose. To this end we remove the transformer structure from the pipeline, thus estimating the final pose from a single image. Table IV presents the results of this experiment for both datasets, STB and MuViHand, with both testing protocols (cross-subject and cross-activity). It can be observed that the performance of our method drops in the absence of learning contextual information, indicating that temporal and multi-view sequences provide additional valuable data points which can be effectively and successfully exploited by the transformer in our model. In particular, the EPE increases by around 25 mm for the STB dataset, and by an average of 7 mm and 27 mm for MuViHand dataset in the cross-subject and cross-activity schemes, respectively.

V. CONCLUSION

We present SeTHPose, a model capable of exploiting sequential hand data (video or multi-view images) using transformers to perform accurate 3D HPE. Our model includes multiple components to encode individual hand frames, learn the sequential contexts, and estimate 3D hand poses. Our model is evaluated by a number of experiments, which include comparisons with state-of-the-art methods using publicly available datasets and ablated baselines. These experiments demonstrate the effectiveness of our method by outperforming other solutions in the area.

REFERENCES

- [1] Leyla Khaleghi, Unal Artan, Ali Etemad, and Joshua A. Marshall. Touchless control of heavy equipment using low-cost hand gesture recognition. *IEEE Internet of Things Magazine*, 5(1):54–57, 2022.
- [2] Bardia Doosti. Hand pose estimation: A survey. *arXiv preprint arXiv:1903.01013*, 2019.
- [3] Weiya Chen, Chenchen Yu, Chenyu Tu, Zehua Lyu, Jing Tang, Shiqi Ou, Yan Fu, and Zhidong Xue. A survey on hand pose estimation with wearable sensors and computer-vision-based methods. *Sensors*, 20(4):1074, 2020.
- [4] James Steven Supančić, Gregory Rogez, Yi Yang, Jamie Shotton, and Deva Ramanan. Depth-based hand pose estimation: methods, data, and challenges. *International Journal of Computer Vision*, 126(11):1180–1198, 2018.
- [5] Rui Li, Zhenyu Liu, and Jianrong Tan. A survey on 3D hand pose estimation: Cameras, methods, and datasets. *Pattern Recognition*, 93:251–272, 2019.
- [6] Christian Zimmermann and Thomas Brox. Learning to estimate 3d hand pose from single rgb images. In *IEEE international conference on Computer Vision*, pages 4903–4911, 2017.
- [7] Umar Iqbal, Pavlo Molchanov, Thomas Breuel Juergen Gall, and Jan Kautz. Hand pose estimation via latent 2.5 d heatmap regression. In *European Conference on Computer Vision*, pages 118–134, 2018.
- [8] Bardia Doosti, Shujon Naha, Majid Mirbagheri, and David J Crandall. Hope-net: A graph-based model for hand-object pose estimation. In *IEEE Conference on Computer Vision and Pattern Recognition*, pages 6608–6617, 2020.
- [9] Yana Hasson, Gul Varol, Dimitrios Tzionas, Igor Kalevtykh, Michael J Black, Ivan Laptev, and Cordelia Schmid. Learning joint reconstruction of hands and manipulated objects. In *IEEE Conference on Computer Vision and Pattern Recognition*, pages 11807–11816, 2019.
- [10] Xiong Zhang, Qiang Li, Hong Mo, Wenbo Zhang, and Wen Zheng. End-to-end hand mesh recovery from a monocular rgb image. In *IEEE International Conference on Computer Vision*, pages 2354–2364, 2019.
- [11] Adnane Boukhayma, Rodrigo de Bem, and Philip HS Torr. 3D hand shape and pose from images in the wild. In *IEEE Conference on Computer Vision and Pattern Recognition*, pages 10843–10852, 2019.
- [12] Shreyas Hampali, Sayan Deb Sarkar, Mahdi Rad, and Vincent Lepetit. Handsformer: Keypoint transformer for monocular 3D pose estimation of hands and object in interaction. *arXiv preprint arXiv:2104.14639*, 2021.
- [13] Lin Huang, Jianchao Tan, Jingjing Meng, Ji Liu, and Junsong Yuan. Hot-net: Non-autoregressive transformer for 3D hand-object pose estimation. In *ACM International Conference on Multimedia*, pages 3136–3145, 2020.
- [14] Kevin Lin, Lijuan Wang, and Zicheng Liu. End-to-end human pose and mesh reconstruction with transformers. In *IEEE Conference on Computer Vision and Pattern Recognition*, pages 1954–1963, 2021.
- [15] Linlin Yang, Shile Li, Dongheui Lee, and Angela Yao. Aligning latent spaces for 3D hand pose estimation. In *IEEE International Conference on Computer Vision*, pages 2335–2343, 2019.
- [16] Adrian Spurr, Jie Song, Seonwook Park, and Otmar Hilliges. Cross-modal deep variational hand pose estimation. In *IEEE Conference on Computer Vision and Pattern Recognition*, pages 89–98, 2018.
- [17] Franziska Mueller, Florian Bernard, Oleksandr Sotnychenko, Dushyant Mehta, Srinath Sridhar, Dan Casas, and Christian Theobalt. Generated hands for real-time 3D hand tracking from monocular rgb. In *IEEE Conference on Computer Vision and Pattern Recognition*, pages 49–59, 2018.
- [18] Paschalis Panteleris, Iason Oikonomidis, and Antonis Argyros. Using a single rgb frame for real time 3D hand pose estimation in the wild. In *IEEE Winter Conference on Applications of Computer Vision*, pages 436–445. IEEE, 2018.
- [19] Liangjian Chen, Shih-Yao Lin, Yusheng Xie, Yen-Yu Lin, Wei Fan, and Xiaohui Xie. Dggn: Depth-image guided generative adversarial networks for disentangling rgb and depth images in 3D hand pose estimation. In *IEEE Winter Conference on Applications of Computer Vision*, pages 411–419, 2020.
- [20] Linlin Yang and Angela Yao. Disentangling latent hands for image synthesis and pose estimation. In *IEEE Conference on Computer Vision and Pattern Recognition*, pages 9877–9886, 2019.
- [21] Moran Li, Yuan Gao, and Nong Sang. Exploiting learnable joint groups for hand pose estimation. *arXiv preprint arXiv:2012.09496*, 2020.
- [22] Lihao Ge, Zhou Ren, Yuncheng Li, Zehao Xue, Yingying Wang, Jianfei Cai, and Junsong Yuan. 3D hand shape and pose estimation from a single rgb image. In *IEEE Conference on Computer Vision and Pattern Recognition*, 2019.
- [23] John Yang, Hyung Jin Chang, Seungeui Lee, and Nojun Kwak. Seqhand: Rgb-sequence-based 3D hand pose and shape estimation. In *European Conference on Computer Vision*, pages 122–139. Springer, 2020.
- [24] Yujun Cai, Lihao Ge, Jun Liu, Jianfei Cai, Tat-Jen Cham, Junsong Yuan, and Nadia Magnenat Thalmann. Exploiting spatial-temporal relationships for 3D pose estimation via graph convolutional networks. In *IEEE International Conference on Computer Vision*, pages 2272–2281, 2019.
- [25] Leyla Khaleghi, Alireza Sepas Moghaddam, Joshua Marshall, and Ali Etemad. Multi-view video-based 3D hand pose estimation. *arXiv preprint arXiv:2109.11747*, 2021.
- [26] Liangjian Chen, Shih-Yao Lin, Yusheng Xie, Yen-Yu Lin, and Xiaohui Xie. Mvhm: A large-scale multi-view hand mesh benchmark for accurate 3D hand pose estimation. In *IEEE Winter Conference on Applications of Computer Vision*, pages 836–845, 2021.
- [27] Ashish Vaswani, Noam Shazeer, Niki Parmar, Jakob Uszkoreit, Llion Jones, Aidan N Gomez, Łukasz Kaiser, and Illia Polosukhin. Attention is all you need. In *Advances in Neural Information Processing Systems*, pages 5998–6008, 2017.
- [28] Alexey Dosovitskiy, Lucas Beyer, Alexander Kolesnikov, Dirk Weissenborn, Xiaohua Zhai, Thomas Unterthiner, Mostafa Dehghani, Matthias Minderer, Georg Heigold, Sylvain Gelly, et al. An image is worth 16x16 words: Transformers for image recognition at scale. *arXiv preprint arXiv:2010.11929*, 2020.
- [29] Salman Khan, Muzammal Naseer, Munawar Hayat, Syed Waqas Zamir, Fahad Shahbaz Khan, and Mubarak Shah. Transformers in vision: A survey. *arXiv preprint arXiv:2101.01169*, 2021.
- [30] Kai Han, Yunhe Wang, Hanting Chen, Xinghao Chen, Jianyuan Guo, Zhenhua Liu, Yehui Tang, An Xiao, Chunjing Xu, Yixing Xu, et al. A survey on visual transformer. *arXiv preprint arXiv:2012.12556*, 2020.
- [31] Jiawei Zhang, Jianbo Jiao, Mingliang Chen, Liangqiong Qu, Xiaobin Xu, and Qingxiong Yang. 3D hand pose tracking and estimation using stereo matching. *arXiv preprint arXiv:1610.07214*, 2016.
- [32] Javier Romero, Dimitrios Tzionas, and Michael J Black. Embodied hands: Modeling and capturing hands and bodies together. *ACM Transactions on Graphics*, 36(6):1–17, 2017.
- [33] Tomas Simon, Hanbyul Joo, Iain Matthews, and Yaser Sheikh. Hand keypoint detection in single images using multiview bootstrapping. In *IEEE Conference on Computer Vision and Pattern Recognition*, pages 1145–1153, 2017.
- [34] Chiara Plizzari, Marco Cannici, and Matteo Matteucci. Skeleton-based action recognition via spatial and temporal transformer networks. *Computer Vision and Image Understanding*, 208:103219, 2021.
- [35] Ce Zheng, Sijie Zhu, Matias Mendieta, Taojiannan Yang, Chen Chen, and Zhengming Ding. 3d human pose estimation with spatial and temporal transformers. *arXiv preprint arXiv:2103.10455*, 2021.
- [36] Shuo Chen, Tan Yu, and Ping Li. Mvt: Multi-view vision transformer for 3d object recognition. *arXiv preprint arXiv:2110.13083*, 2021.
- [37] Hui Shuai, Lele Wu, and Qingshan Liu. Adaptively multi-view and temporal fusing transformer for 3D human pose estimation. *arXiv preprint arXiv:2110.05092*, 2021.
- [38] Kaiming He, Xiangyu Zhang, Shaoqing Ren, and Jian Sun. Deep residual learning for image recognition. In *IEEE Conference on Computer Vision and Pattern Recognition*, pages 770–778, 2016.
- [39] Olga Russakovsky, Jia Deng, Hao Su, Jonathan Krause, Sanjeev Satheesh, Sean Ma, Zhiheng Huang, Andrej Karpathy, Aditya Khosla, Michael Bernstein, et al. Imagenet large scale visual recognition challenge. *International journal of Computer Cision*, 115(3):211–252, 2015.
- [40] Thomas N Kipf and Max Welling. Semi-supervised classification with graph convolutional networks. *arXiv preprint arXiv:1609.02907*, 2016.